RESEARCH ARTICLE

Check for updates

Light-activatable photochemically targeting chimeras (PHOTACs) enable the optical control of targeted protein degradation of HDAC6†

Silas L. Wurnig,‡[a] Maria Hanl,‡[a] Thomas M. Geiger,[b] Shiyang Zhai,[a] Ina Dressel,[b] Dominika E. Pieńkowska,[b] Radosław P. Nowak[b] and Finn K. Hansen ![ORCID] *[a]

Proteolysis targeting chimeras (PROTACs) are heterobifunctional modalities that induce protein degradation *via* a catalytic mode of action. Photochemically targeting chimeras (PHOTACs) are a subset of PROTACs designed for light-activated protein degradation, thereby offering precise spatiotemporal control. In this study, we report the design, solid-phase synthesis, and characterization of the first PHOTACs targeting histone deacetylase 6 (HDAC6). We achieved this by incorporating an azobenzene photoswitch into our previously developed HDAC6-selective PROTAC **A6**. Among the synthesized compounds, PHOTAC **12** demonstrated no HDAC6 degradation in the absence of light but showed significant degradation upon activation to its *cis*-state with 390 nm light irradiation. Notably, we find that PHOTAC **12** in the *cis*-state shows significantly improved ternary complex formation compared to the *trans*-state correlating with its degradation efficacy. Overall, PHOTAC **12** is a promising lead compound for the development of light-activatable HDAC6 degraders.

Introduction

Proteolysis targeting chimeras (PROTACs) have become a leading technology in targeted protein degradation.[1] These molecules consist of three moieties: a protein of interest (POI) ligand and an E3 ligase ligand tethered by a linker. PROTACs induce proximity between the POI and the E3 ligase, thereby resulting in efficient ubiquitin transfer and polyubiquitination of the target protein.[2] This ubiquitination then serves as recognition for the proteasome and the polyubiquitinated protein is subsequently degraded by the proteasome.[3] Therefore, PROTACs act as catalysts and can participate in successive ternary complex formations. This approach offers various advantages over traditional occupancy-driven therapeutic modalities. While occupancy-driven approaches need extensive optimization of the ligand to ensure adequate physiological effects, PROTACs often do not need high affinity towards their POI due to the catalytic mode of action.[4]

Additionally, the POI ligand moiety of PROTACs does not necessarily have to bind to an active site of a protein. The POI can be targeted at any pocket addressable by a small molecule ligand, thereby reducing the competition with endogenous ligands, which usually necessitates high affinity of the ligands to the target protein.[5] With the first PROTACs entering late-stage clinical trials, there is growing interest in the exploration of new methodologies to expand the toolkit for targeted protein degradation. To broaden the scope of targeted protein degradation, innovative approaches such as molecular glues, lysosome targeting chimeras (LYTACs), autophagy targeting chimeras (AUTACs), and antibody targeted chimeras (AbTACs) have emerged as promising strategies.[6–9]

While these novel methods have expanded the range of proteins that can be targeted, they have limitations in terms of spatial and temporal control of their activity. Once administered, these degraders typically act continuously, degrading target proteins regardless of their physiological context or location, which can lead to unwanted toxicity.[10] Despite their versatility, the lack of precise modulation of protein function remains a challenge for therapeutic applications.

One approach to achieve localized drug effects is through light control. The use of light to precisely modulate biological pathways has gained attention in recent years.[11,12] Optical control methods include, among others, photocaged compounds and synthetic photoswitches, which use photochemical isomerization and thermal relaxation processes

[a] Department of Pharmaceutical and Cell Biological Chemistry, Pharmaceutical Institute, University of Bonn, An der Immenburg 4, 53121 Bonn, Germany. E-mail: finn.hansen@uni-bonn.de

[b] Institute of Structural Biology, Medical Faculty, University of Bonn, Venusberg Campus 1, 53127 Bonn, Germany
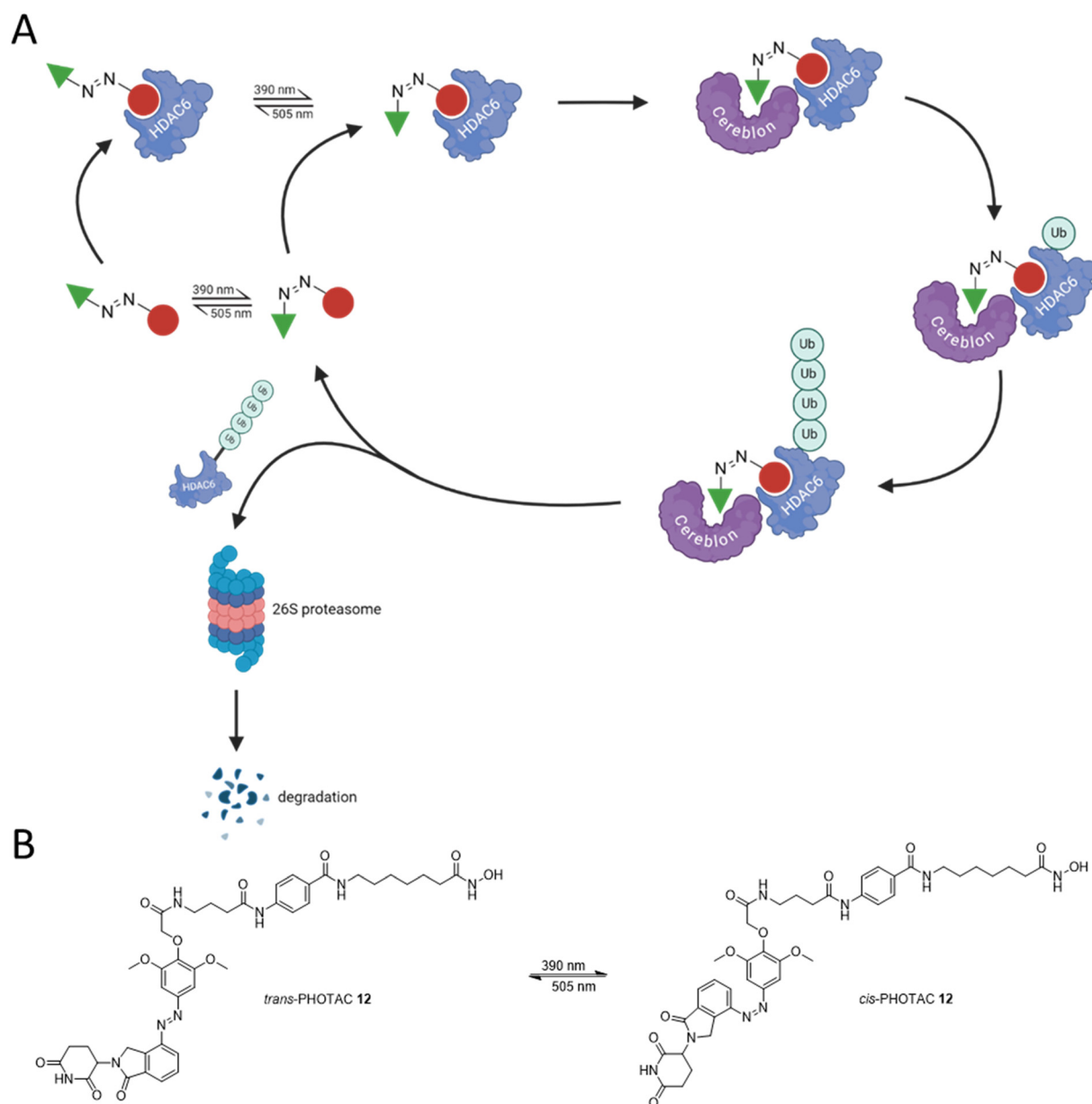
† Electronic supplementary information (ESI) available: Supplemental figures, experimental procedures, ^{1}H and 13C NMR data, and HPLC chromatograms. See DOI: https://doi.org/10.1039/d4md00972j

‡ S. L. W. and M. H. contributed equally and share the first authorship.

to alter compound activity, thereby providing precise temporal and spatial control over their effects.[13–18]

In 2020, Trauner and co-workers introduced the first photochemically targeting chimeras (PHOTACs).[10] These molecules are light-activatable PROTACs and consist of a POI ligand, a photoswitch, and an E3 ligase ligand. In their inactive form, PHOTACs prevent ternary complex formation by introducing a steric clash between the binary complex and the second protein (Fig. 1A).[10] When irradiated with light of a specific wavelength, the internal photoswitch changes its conformation, enabling the PHOTAC to form a productive ternary complex (Fig. 1A and B). This leads to polyubiquitination and subsequent proteasomal degradation

of the POI. The active isomer gradually reverts to the inactive form through thermal relaxation, losing its activity, and can also be rapidly inactivated photochemically.[18] This approach could potentially minimize adverse effects, as PHOTACs can be selectively activated by light at the desired location. Their inactivation is also less dependent on clearance and metabolism. Thus, PHOTACs provide a level of spatiotemporal and local control that is unmatched by other targeted protein degradation methods. In this study, we synthesized and characterized a set of three PHOTACs for targeted HDAC6 degradation by incorporating an azobenzene photoswitch, using our previously published HDAC6 PROTAC **A6** as a template (Fig. 2).[19]

Fig. 1 (A) Mechanism of an HDAC6 targeting PHOTAC. After illumination with the appropriate wavelength, the PHOTAC switches from the *trans*-to the *cis*-isomer resulting in increased ternary complex formation. Successful ternary complex formation leads to the polyubiquitination of the targeted protein and proteosomal degration. (B) Switching of a PHOTAC from the *trans*- to the *cis*-isomer. Created with BioRender.
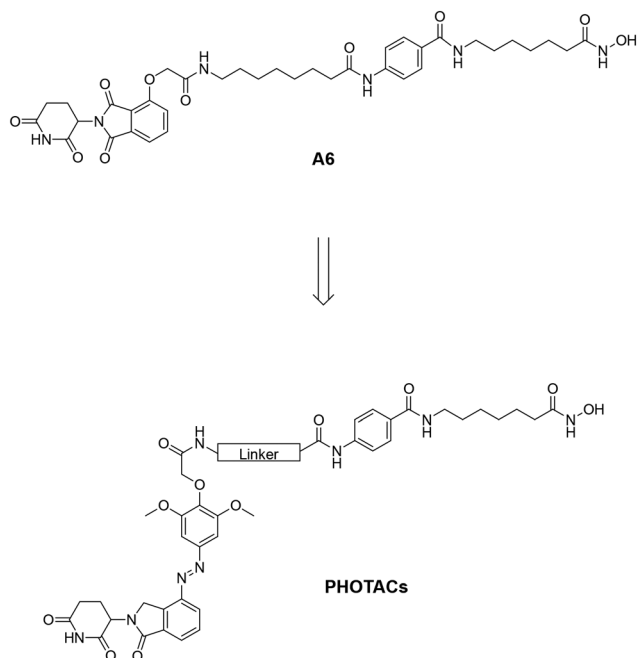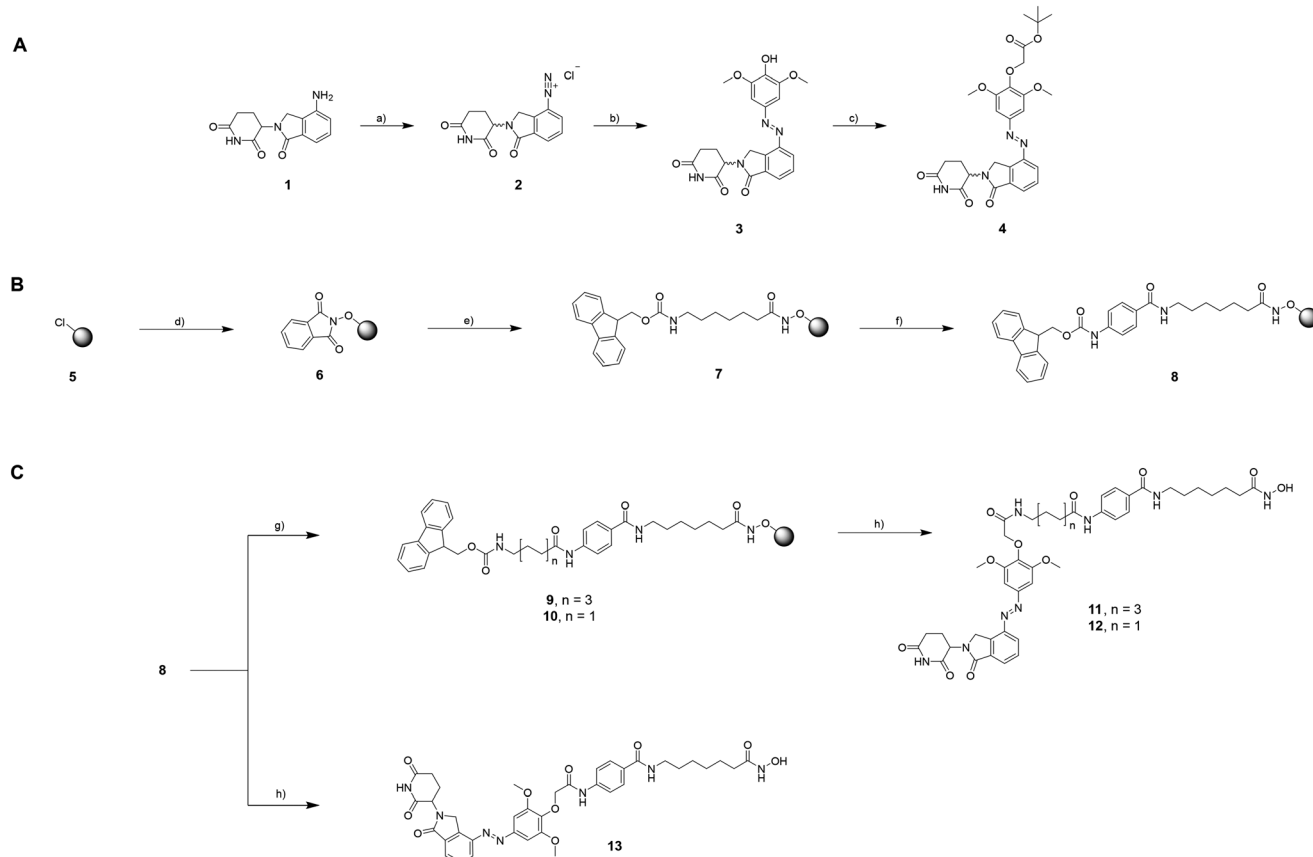
Fig. 2 Design of the PHOTACs based on the existing HDAC6 degrader **A6**.[19]

Results and discussion

The thalidomide moiety of **A6** was replaced by a photoswitchable lenalidomide-based cereblon (CRBN)-recruiter to obtain the desired PHOTACs. The synthesis of the photoswitch (outlined in Scheme 1A) was performed by dissolving lenalidomide (**1**) in hydrochloric acid followed by the addition of sodium nitrite to obtain the aryldiazonium salt **2**. This intermediate was then exposed to a solution of 2,6-dimethoxyphenol to obtain the diazo compound **3**. In the next step, compound **3** was treated with *tert*-butyl bromoacetate to obtain the photoswitchable CRBN ligand **4** *via* a nucleophilic substitution reaction.

The synthesis of the HDAC ligand was performed on a 2-chlorotrityl chloride (2-CTC) resin. Firstly, the commercially available 2-CTC resin (**5**) was treated with *N*-hydroxyphthalimide to obtain the protected immobilized hydroxylamine **6**. In the next step, the phthalimide protecting group was cleaved by treatment with hydrazine hydrate and the subsequent HATU-mediated amide coupling with Fmoc-7-aminoheptanoic acid gave the intermediate **7**. Subsequent Fmoc-deprotection by treatment with a piperidine solution and HATU-mediated

Scheme 1 Reagents and conditions: (A) a) HBF₄, NaNO₂, HCl, 0 °C, 1 h; b) 2,6-dimethoxyphenol, NaHCO₃, Na₂CO₃, H₂O, MeOH, 0 °C, 1 h; c) *tert*-butyl bromoacetate, K₂CO₃, DMF, rt, 4 h. (B) d) *N*-Hydroxyphthalimide, DIPEA, DMF, 16 h; e) hydrazine hydrate, Fmoc-7-aminoheptanoic acid, HATU, HOBt, DIPEA, DMF, rt, 16 h; f) (i) 20% piperidine, DMF, 2 × 5 min; (ii) Fmoc-4-aminobenzoic acid, HATU, HOBt, DIPEA, DMF, rt, 16 h; (C) g) (i) 20% piperidine, DMF, 2 × 5 min; (ii) Fmoc-4-aminobutanoic acid/Fmoc-8-aminooctanoic acid, HATU, HOBt, DIPEA, DMF, rt, 16 h; h) (i) **4**, TFA, DCM, rt, 4 h; (ii) 20% piperidine, DMF, rt, 20 min; (iii) HATU, HOBt, DIPEA, DMF, rt, 16 h.
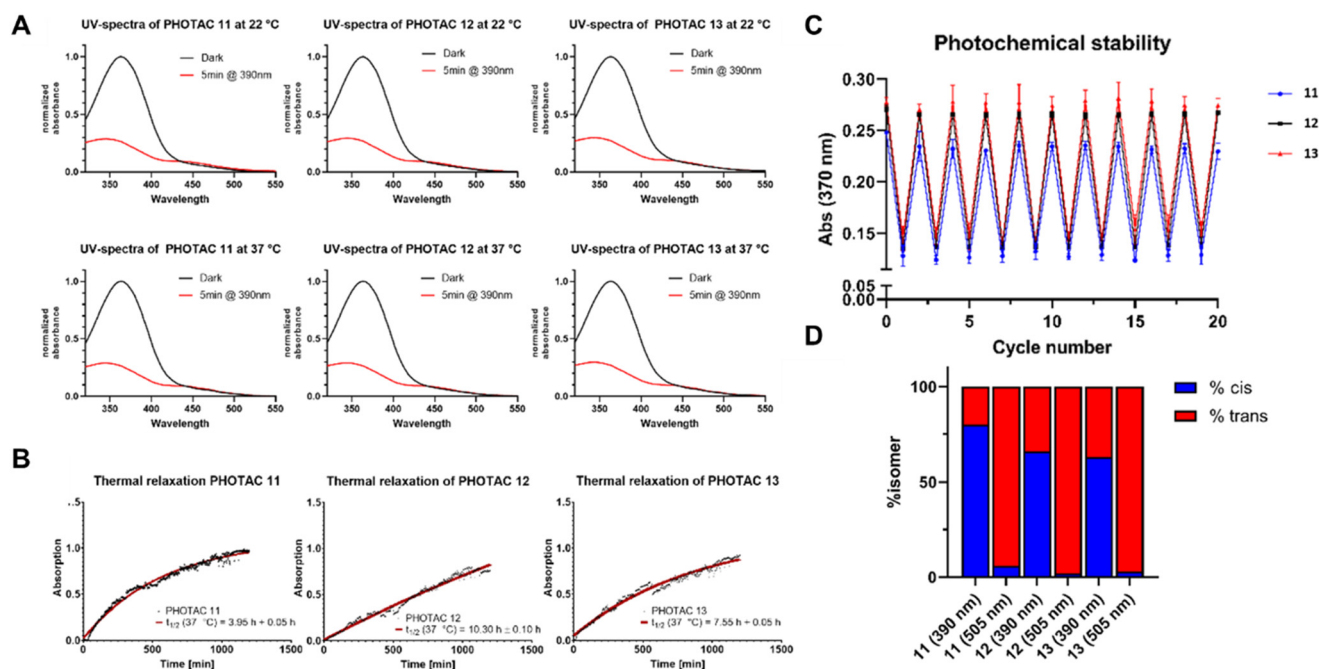
amide coupling with Fmoc-4-aminobenzoic acid yielded the resin-bound key intermediate **8** (Scheme 1B). From this point, the diversification of linker length was introduced in the last steps (Scheme 1C). To this end, the Fmoc-protecting group of **8** was cleaved and the subsequent HATU-mediated amide coupling with either Fmoc-8-aminooctanoic acid or Fmoc-4-aminobutanoic acid yielded the PHOTAC precursors **9** and **10**. In the last step of the synthesis, the photoswitchable CRBN ligand **4** and the intermediates **8**, **9**, and **10** were subjected to an HATU-mediated amide coupling to obtain the final PHOTACs **11**–**13**. First, the CRBN ligand **4** was converted into the corresponding carboxylic acid by treatment with trifluoroacetic acid (TFA). The resin-bound HDAC6 ligands **8**, **9** and **10** were then Fmoc-deprotected followed by an amide coupling with the photoswitchable CRBN ligand. After the successful amide coupling reactions, the products were cleaved from the resin and purified by preparative HPLC to yield the PHOTACs **11**–**13** in > 95% purity. The positive control **A6** was synthesized according to our previously published procedure.[19]

The most important step in the photochemical evaluation of the synthesized PHOTACs was to confirm their ability to switch from the *trans*- to the *cis*-state. In order to investigate this, the UV spectra of the respective PHOTACs **11**–**13** were measured in the dark. After illumination with light at a wavelength of 390 nm, the UV spectra were measured again, and the two distinct spectra were overlaid (Fig. 3A). This experiment was performed at a room temperature of 22 °C and at the physiological temperature of 37 °C. All synthesized PHOTACs showed the same overlaid spectra regardless of the temperature, confirming their intrinsic ability to switch from the *trans*- to the *cis*-state
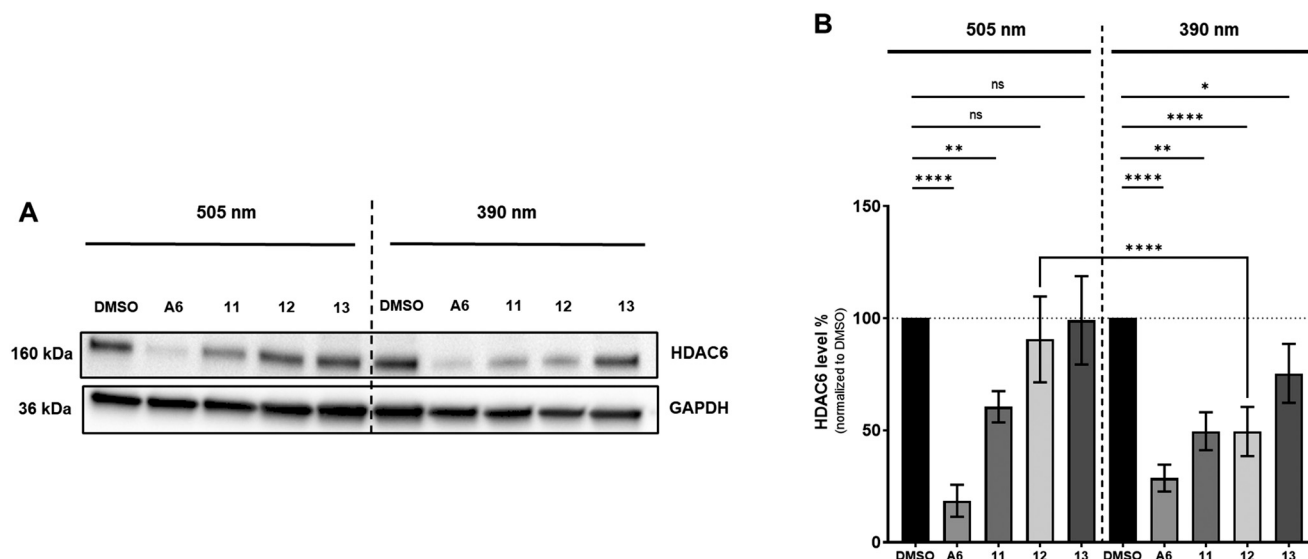
independently of temperature. This ensures the possibility for a cellular use of the synthesized PHOTACs.

To investigate whether the photoactivated PHOTACs show a half-life long enough to induce degradation of the target protein, the half-lifes of PHOTACs **11**–**13** were measured photometrically. To this end, the absorbance at 370 nm was measured prior to illumination for normalization. After irradiation with the appropriate wavelength for 5 minutes the absorbance at 370 nm was measured over a time period of 20 hours at a temperature of 37 °C to calculate the respective half-life times of the *cis*-isomers at physiological temperatures. The results are shown in Fig. 3B. PHOTAC **12** showed the longest half-life with 10.30 h, while the PHOTACs **11** and **13** demonstrated shorter half-life times of 3.95 h and 7.55 h, respectively. The photochemical stability of the synthesized PHOTACs was then tested by rapidly switching them between the *cis*- and the *trans*-state and measuring the absorbance at 370 nm. All three PHOTACs showed no change in absorbance at both states over the course of 20 cycles ensuring the stability of the photoswitch (Fig. 3C). Lastly the amount of *cis*- and *trans*-isomers at the photostationary states (PSSs) were measured photometrically. All three PHOTACs showed a photostationary state containing 63–80% of the *cis*-isomer after irradiation at 390 nm and could be switched back to >94% of *trans*-isomer following irradiation at 505 nm (Fig. 3D).

In the next step, we evaluated the ability of PHOTACs **11**–**13** to degrade HDAC6 using PROTAC **A6** as positive control. To this end, we treated MM.1S cells with 1 μM of **11**–**13** or **A6** for 6 hours. The MM.1S cell line was selected due to its well-established use in PROTAC characterization and our prior

Fig. 3 (A) Overlaid UV-vis spectra of the *cis*- and *trans*-state PHOTACs **11**–**13** at 22 °C and 37 °C in DMSO. (B) Thermal relaxation measurements of the synthesized PHOTACs **11**–**13**. (C) Photochemical stability of the synthesized PHOTACs **11**–**13** over 20 cycles of switching between the *cis*- and the *trans*-isomer. (D) Percentage of *cis*- and *trans*-isomer of PHOTACs **11**–**13** after irradiation with 390 nm and 505 nm.
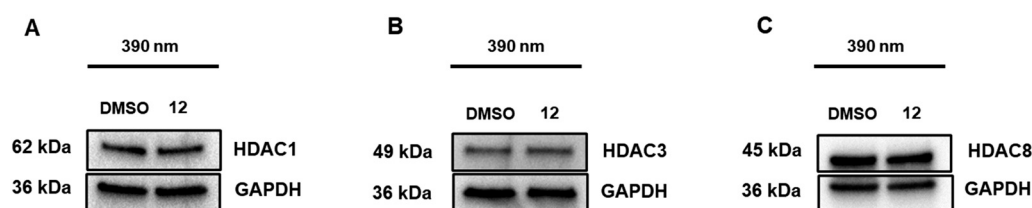
Fig. 4 Immunoblot analysis of HDAC6 levels in MM1.S cells after irradiation with 390 nm or 505 nm. Afterwards, the cells were irradiated every hour for 30 seconds at 390 nm (390 nm group) or kept in the dark (505 nm group) and incubated for 6 h at 37 °C under humidified air with 5% CO_2. (A) Representative immunoblot of HDAC6 and GAPDH protein levels in MM1.S cells treated with 1 μM of compounds **A6**, **11**, **12**, and **13** for 6 hours. (B) Densiometric analysis of the immunoblots normalized to vehicle control (DMSO). Data are presented as mean ± SD ($n \geq 4$ replicates). ns = not significant, * $p < 0.1$, ** $p < 0.01$, **** $p < 0.0001$, determined by unpaired t test with Welch's correction.

findings demonstrating **A6**'s high degradation activity in these cells.[20,21] The experiments were conducted in two treatment groups. Both treatment groups were first treated with light of 505 nm to ensure full conversion into the *trans*-state. Next, one group was kept in the dark, and the second group was treated with light of 390 nm to switch the PHOTACs into the *cis*-state (see ESI† for experimental details; the results are summarized in Fig. 4). The positive control **A6** achieved significant HDAC6 degradation after treatment with 390 and 505 nm. PHOTAC **11** induced HDAC6 degradation after irradiation with both wavelengths, likely due to its relatively long and flexible linker. The linker-less PHOTAC **13** failed to degrade HDAC6 in both treatment groups. In contrast, PHOTAC **12** with a relatively short γ-aminobutyric acid linker was unable to degrade HDAC6 after irradiation with 505 nm ($<10\%$ D_{max}) but showed a pronounced and significant degradation of HDAC6 with a D_{max} of ~50% at 1 μM concentration upon irradiation with light of 390 nm. These results indicate that the *cis*-state of PHOTAC **12** is an active degrader, while the *trans*-state is nearly inactive ($<10\%$ D_{max}).

Subsequently, we analyzed the HDAC degradation selectivity profile of **12** after activation to its *cis*-state by irradiation with light of 390 nm. Consistent with its parent PROTAC **A6**,[19] activated PHOTAC **12** selectively degraded HDAC6 while causing minimal degradation of HDAC1, HDAC3, and HDAC8 (Fig. 5). Similarly, when preirradiated with 505 nm to ensure the *trans*-form, PHOTAC **12** did not induce degradation of HDAC1, HDAC3, or HDAC8 (Fig. S1, ESI†).

After confirming that **12** can be activated by treatment with light of 390 nm into an active and selective HDAC6 degrader, we analyzed the concentration dependency of **12**-mediated HDAC6 degradation. To this end, we treated MM.1S cells with varying concentrations of **12** (0.123, 0.37, 1.11, 3.33, and 10 μM) and determined the resulting HDAC6 protein levels by immunoblot analysis. The maximum degradation was observed at a concentration of 0.37 μM and the HDAC6 protein levels remained stable up to the highest tested concentration (see Fig. S2, ESI†).

To further investigate the mode of action and confirm the expected degradation mechanism, we conducted co-treatment

Fig. 5 Immunoblot analysis of HDAC isoform levels in MM1.S after irradiation with 390 nm. MM.1S cells were treated with **12** (1 μM) or vehicle (DMSO) for 6 h. HDAC1 (A), HDAC3 (B), and HDAC8 (C) levels were analyzed by immunoblotting. GAPDH was used as loading control. Representative images from a total of $n = 2$ replicates.
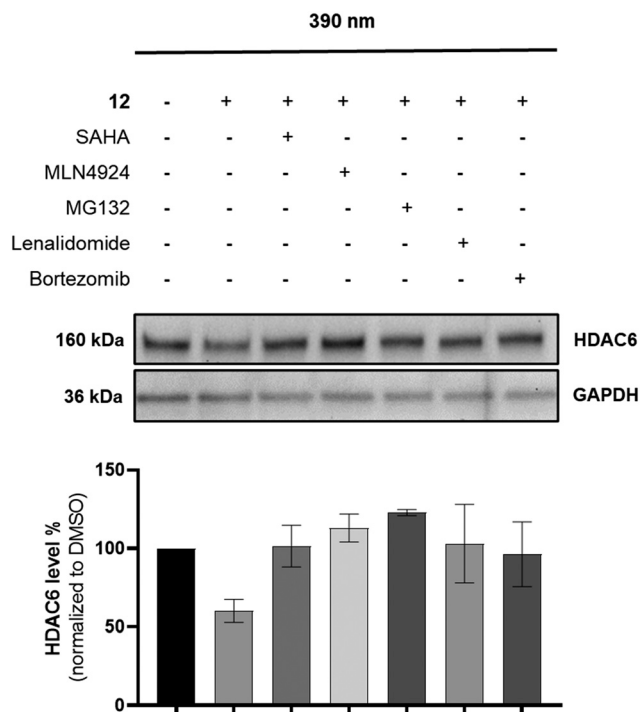
Fig. 6 Immunoblot analysis of HDAC6 levels in MM1.S after treatment with **12** (1 μM) after 6 h incubation after irradiation with 390 nm. MM.1S cells were co-treated with vorinostat (SAHA, 1 μM), MLN4924 (1 μM), MG132 (1 μM), lenalidomide (5 μM), or bortezomib (0.5 μM) for 6 h. HDAC6 levels were analyzed by immunoblotting. GAPDH was used as loading control. Representative images from a total of $n = 2$ replicates.

experiments of activated **12** with the HDAC inhibitor vorinostat (SAHA, 1 μM), neddylation inhibitor MLN4924 (1 μM), CRBN ligand lenalidomide (5 μM), and the proteasome inhibitors MG132 (1 μM), and bortezomib (0.5 μM). In all co-treatment conditions, the HDAC6 levels increased (see Fig. 6), indicating that HDAC6 degradation requires the binding of **12** to both

HDAC6 and CRBN and is neddylation- and proteasome-dependent.

To explore the differential activities of the *cis*- and *trans*-state of PHOTAC **12**, we monitored ternary complex formation through TR-FRET between purified CRBN-DDB1ΔB and HDAC6. After irradiation with 390 nm light (*cis*-state), PHOTAC **12** led to approximately 2-fold increase in ternary complex between CRBN and HDAC6 compared to 505 nm condition (*trans*-state) (Fig. 7A), which explains the reduced degradation in a cellular environment. Our prior experiments showed that 390 nm irradiation results in ~65% transition to *cis*-state (Fig. 3D), while 505 nm light results in near 95% transition to *trans*-state indicating that the pure *cis*-state would result in even higher ternary complex formation. To gain deeper insights on a molecular level, we performed modeling studies utilizing an established protocol for ternary complex modeling.[22,23] To this end, crystal structures of HDAC6 (PDB ID: 5EEI)[24] and CRBN (PDB ID: 4CI2)[25] were selected as templates. The results (Fig. 7B) demonstrate that both *cis*- and *trans*-states of PHOTAC **12** are capable of forming distinct ternary complexes with HDAC6 and CRBN. Specifically, the HDAC warhead in both states of PHOTAC **12** engages in metal chelation with Zn^{2+} within the HDAC6 pocket. In addition, the CRBN warhead of PHOTAC **12** in both states forms hydrogen bonds with N353, H380, and W382 within the CRBN binding pocket, which are crucial for CRBN recruitment. These interactions provide the basis for ternary complex formation and corroborate the findings from immunoblot analysis and TR-FRET assay.

Conclusions

In conclusion, in this study we successfully designed, synthesized, and characterized the first photochemically targeting chimeras (PHOTACs) for the targeted degradation of histone deacetylase 6 (HDAC6). By incorporating an azobenzene photoswitch into our previously developed HDAC6-selective
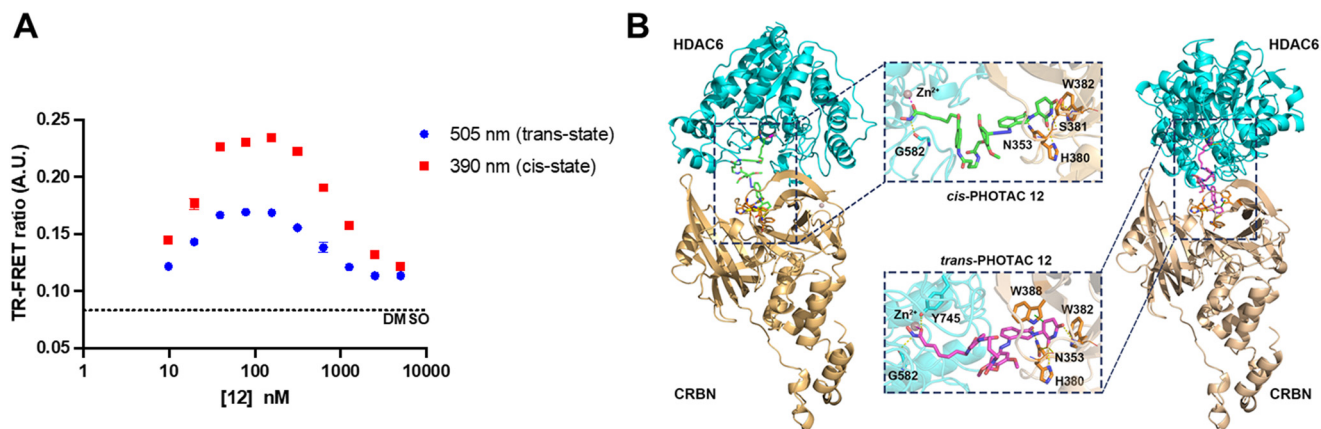

Fig. 7 (A) TR-FRET ternary complex formation between CRBN-DDB1ΔB and HDAC6 in presence of PHOTAC **12** after irradiation of light at a wavelength of 390 nm or 505 nm. Data is shown as mean ± SD interval of $n = 2$ replicates. The dashed line indicates the baseline signal in the DMSO only well. (B) Ternary complex modeling of HDAC6-*cis*-PHOTAC **12**-CRBN and HDAC6-*trans*-PHOTAC **12**-CRBN. HDAC6 is shown in cyan and CRBN in wheat. Hydrogen bonds are shown as yellow dashes, H−π interactions are shown as green dashes and metal chelation is indicated as purple dashes.

PROTAC **A6**, we created PHOTAC **12**, which exhibited significant HDAC6 degradation only upon activation to its *cis*-state by irradiation with light of 390 nm. *In vitro* ternary complex dimerization assay indicated that the *cis*-isomer of PHOTAC **12** results in significant increase in ternary complex formed, consistent with potent degradation of HDAC6. These findings establish PHOTAC **12** as a promising lead for the development of light-activatable HDAC6 degraders, highlighting the potential of PHOTACs for the precise spatiotemporal control in targeted protein degradation.

Data availability

The data supporting this article have been included as part of the ESI.†

Author contributions

The manuscript was written through contributions of all authors. All authors have given approval to the final version of the manuscript.

Conflicts of interest

There are no conflicts to declare.

Acknowledgements

References

1 M. Békés, D. R. Langley and C. M. Crews, PROTAC targeted protein degraders: the past is prologue, *Nat. Rev. Drug Discovery*, 2022, **21**(3), 181–200, DOI: **10.1038/s41573-021-00371-6**.

2 Z. Liu, M. Hu, Y. Yang, C. Du, H. Zhou, C. Liu, Y. Chen, L. Fan, H. Ma, Y. Gong and Y. Xie, An overview of PROTACs: a promising drug discovery paradigm, *Mol. Biomed.*, 2022, **3**(1), 46, DOI: **10.1186/s43556-022-00112-0**.

3 G. L. Grice and J. A. Nathan, The recognition of ubiquitinated proteins by the proteasome, *Cell. Mol. Life Sci.*, 2016, **73**(18), 3497–3506, DOI: **10.1007/s00018-016-2255-5**.

4 H. Graham, The mechanism of action and clinical value of PROTACs: A graphical review, *Cell. Signalling*, 2022, **99**, 110446, DOI: **10.1016/j.cellsig.2022.110446**.

5 V. Haridas, S. Dutta, A. Munjal and S. Singh, Inhibitors to degraders: Changing paradigm in drug discovery, *iScience*, 2024, **27**(5), 109574, DOI: **10.1016/j.isci.2024.109574**.

6 A. D. Cotton, D. P. Nguyen, J. A. Gramespacher, I. B. Seiple and J. A. Wells, Development of Antibody-Based PROTACs for the Degradation of the Cell-Surface Immune Checkpoint Protein PD-L1, *J. Am. Chem. Soc.*, 2021, **143**(2), 593–598, DOI: **10.1021/jacs.0c10008**.

7 J. M. Sasso, R. Tenchov, D. Wang, L. S. Johnson, X. Wang and Q. A. Zhou, Molecular Glues: The Adhesive Connecting Targeted Protein Degradation to the Clinic, *Biochemistry*, 2023, **62**(3), 601–623, DOI: **10.1021/acs.biochem.2c00245**.

8 Q. Zheng, J. Guo, R. Ma and W. Pu, Lysosome-targeting Chimera (LYTAC): A Silver Bullet for Targeted Degradation of Oncogenic Membrane Proteins, *MedComm: Oncol.*, 2024, **3**(1), 2–5, DOI: **10.1002/mog2.64**.

9 L. Zhao, J. Zhao, K. Zhong, A. Tong and D. Jia, Targeted protein degradation: mechanisms, strategies and application, *Signal Transduction Targeted Ther.*, 2022, **7**(1), 113, DOI: **10.1038/s41392-022-00966-4**.

10 M. Reynders, B. S. Matsuura, M. Bérouti, D. Simoneschi, A. Marzio, M. Pagano and D. Trauner, PHOTACs enable optical control of protein degradation, *Sci. Adv.*, 2020, **6**(8), eaay5064, DOI: **10.1126/sciadv.aay5064**.

11 L. Z. Fan and M. Z. Lin, Optical control of biological processes by light-switchable proteins, *Wiley Interdisc. Rev.: Dev. Biol.*, 2015, **4**(5), 545–554, DOI: **10.1002/wdev.188**.

12 N. Ankenbruck, T. Courtney, Y. Naro and A. Deiters, Optochemical Control of Biological Processes in Cells and Animals, *Angew. Chem., Int. Ed.*, 2018, **57**(11), 2768–2798, DOI: **10.1002/anie.201700171**.

13 P. Pfaff, K. T. G. Samarasinghe, C. M. Crews and E. M. Carreira, Reversible Spatiotemporal Control of Induced Protein Degradation by Bistable PhotoPROTACs, *ACS Cent. Sci.*, 2019, **5**(10), 1682–1690, DOI: **10.1021/acscentsci.9b00713**.

14 F. B. Kraft, M. Hanl, F. Feller, L. Schäker-Hübner and F. K. Hansen, Photocaged Histone Deacetylase Inhibitors as Prodrugs in Targeted Cancer Therapy, *Pharmaceuticals*, 2023, **16**(3), 356, DOI: **10.3390/ph16030356**.

15 R. Chen, Z. Wang, L. Liu and Z. Pan, Discovery of novel photocaged ERK1/2 inhibitors as light-controlled anticancer agents, *Chem. Commun.*, 2022, **58**(31), 4901–4904, DOI: **10.1039/D2CC00456A**.

16 Q. Zhang, C. S. Kounde, M. Mondal, J. L. Greenfield, J. R. Baker, S. Kotelnikov, M. Ignatov, C. P. Tinworth, L. Zhang, D. Conole, E. de, D. Kozakov, A. McCluskey, J. D. Harling, M. J. Fuchter and E. W. Tate, Light-mediated multi-target protein degradation using arylazopyrazole photoswitchable PROTACs (AP-PROTACs), *Chem. Commun.*, 2022, **58**(78), 10933–10936, DOI: **10.1039/D2CC03092F**.

17 J. Cheng, J. Zhang, S. He, M. Li, G. Dong and C. Sheng, Photoswitchable PROTACs for Reversible and Spatiotemporal Regulation of NAMPT and NAD, *Angew. Chem.*, 2024, **63**(12), e202315997, DOI: **10.1002/anie.202315997**.

18 T. Ko, C. Jou, A. B. Grau-Perales, M. Reynders, A. A. Fenton and D. Trauner, Photoactivated Protein Degrader for Optical

Control of Synaptic Function, *ACS Chem. Neurosci.*, 2023, **14**(19), 3704–3713, DOI: **10.1021/acschemneuro.3c00390**.

19 L. Sinatra, J. Yang, J. Schliehe-Diecks, N. Dienstbier, M. Vogt, P. Gebing, L. M. Bachmann, M. Sönnichsen, T. Lenz, K. Stühler, A. Schöler, A. Borkhardt, S. Bhatia and F. K. Hansen, Solid-Phase Synthesis of Cereblon-Recruiting Selective Histone Deacetylase 6 Degraders (HDAC6 PROTACs) with Antileukemic Activity, *J. Med. Chem.*, 2022, **65**(24), 16860–16878, DOI: **10.1021/acs.jmedchem.2c01659**.

20 F. Feller, I. Honin, M. Miranda, H. Weber, S. Henze, M. Hanl and F. K. Hansen, Development of the First-in-Class FEM1B-Recruiting Histone Deacetylase Degraders, *J. Med. Chem.*, 2025, **68**(2), 1824–1843, DOI: **10.1021/acs.jmedchem.4c02569**.

21 C. Steinebach, A. Bricelj, A. Murgai, I. Sosič, L. Bischof, Y. L. D. Ng, C. Heim, S. Maiwald, M. Proj, R. Voget, F. Feller, J. Košmrlj, V. Sapozhnikova, A. Schmidt, M. R. Zuleeg, P. Lemnitzer, P. Mertins, F. K. Hansen, M. Gütschow, J. Krönke and M. D. Hartmann, Leveraging Ligand Affinity and Properties: Discovery of Novel Benzamide-Type Cereblon Binders for the Design of PROTACs, *J. Med. Chem.*, 2023, **66**(21), 14513–14543, DOI: **10.1021/acs.jmedchem.3c00851**.

22 M. L. Drummond and C. I. Williams, In Silico Modeling of PROTAC-Mediated Ternary Complexes: Validation and Application, *J. Chem. Inf. Model.*, 2019, **59**(4), 1634–1644, DOI: **10.1021/acs.jcim.8b00872**.

23 M. L. Drummond, A. Henry, H. Li and C. I. Williams, Improved Accuracy for Modeling PROTAC-Mediated Ternary Complex Formation and Targeted Protein Degradation via New In Silico Methodologies, *J. Chem. Inf. Model.*, 2020, **60**(10), 5234–5254, DOI: **10.1021/acs.jcim.0c00897**.

24 Y. Hai and D. W. Christianson, Histone deacetylase 6 structure and molecular basis of catalysis and inhibition, *Nat. Chem. Biol.*, 2016, **12**(9), 741–747, DOI: **10.1038/nchembio.2134**.

25 E. S. Fischer, K. Böhm, J. R. Lydeard, H. Yang, M. B. Stadler, S. Cavadini, J. Nagel, F. Serluca, V. Acker, G. M. Lingaraju, R. B. Tichkule, M. Schebesta, W. C. Forrester, M. Schirle, U. Hassiepen, J. Ottl, M. Hild, R. E. J. Beckwith, J. W. Harper, J. L. Jenkins and N. H. Thomä, Structure of the DDB1-CRBN E3 ubiquitin ligase in complex with thalidomide, *Nature*, 2014, **512**(7512), 49–53, DOI: **10.1038/nature13527**.